energies

MDPI

Article

An Experimental Study of the Possibility of In Situ Hydrogen Generation within Gas Reservoirs

Pavel Afanasev [1,*], Evgeny Popov [1], Alexey Cheremisin [1], Roman Berenblyum [2], Evgeny Mikitin [3], Eduard Sorokin [3], Alexey Borisenko [3], Viktor Darishchev [4], Konstantin Shchekoldin [4] and Olga Slavkina [4]

[1] Skolkovo Institute of Science and Technology, 121205 Moscow, Russia; e.popov@skoltech.ru (E.P.); a.cheremisin@skoltech.ru (A.C.)
[2] Hydrogen Source AS, 0114 Oslo, Norway; roman.berenblyum@hydrogen-source.com
[3] Lukoil Engineering LLC, 109028 Moscow, Russia; Evgenij.Mikitin@lukoil.com (E.M.); Eduard.Sorokin@lukoil.com (E.S.); Alexey.Borisenko@lukoil.com (A.B.)
[4] Ritek LLC, 400048 Volgograd, Russia; Viktor.Darischev@lukoil.com (V.D.); Konstantin.Schekoldin@lukoil.com (K.S.); olga.slavkina@lukoil.com (O.S.)
* Correspondence: pavel.afanasev@skoltech.ru

Abstract: Hydrogen can be generated in situ within reservoirs containing hydrocarbons through chemical reactions. This technology could be a possible solution for low-emission hydrogen production due to of simultaneous CO_2 storage. In gas fields, it is possible to carry out the catalytic methane conversion (CMC) if sufficient amounts of steam, catalyst, and heat are ensured in the reservoir. There is no confirmation of the CMC's feasibility at relatively low temperatures in the presence of core (reservoir rock) material. This study introduces the experimental results of the first part of the research on in situ hydrogen generation in the Promyslovskoye gas field. A set of static experiments in the autoclave reactor were performed to study the possibility of hydrogen generation under reservoir conditions. It was shown that CMC can be realized in the presence of core and ex situ prepared Ni-based catalyst, under high pressure up to 207 atm, but at temperatures not lower than 450 °C. It can be concluded that the crushed core model improves the catalytic effect but releases carbon dioxide and light hydrocarbons, which interfere with the hydrogen generation. The maximum methane conversion rate to hydrogen achieved at 450 °C is 5.8%.

Keywords: hydrogen production; steam methane reforming; in situ hydrogen generation

Citation: Afanasev, P.; Popov, E.; Cheremisin, A.; Berenblyum, R.; Mikitin, E.; Sorokin, E.; Borisenko, A.; Darishchev, V.; Shchekoldin, K.; Slavkina, O. An Experimental Study of the Possibility of In Situ Hydrogen Generation within Gas Reservoirs. *Energies* **2021**, *14*, 5121. https://doi.org/10.3390/en14165121

Academic Editor: Bahman Shabani

Received: 21 July 2021
Accepted: 16 August 2021
Published: 19 August 2021

1. Introduction

The growing demand for clean energy resources stimulates the development of unconventional and alternative energy. Renewable energy is a promising and developing field, but hydrogen has a number of benefits as an energy source. According to the world's long-term programs for developing hydrogen technologies, hydrogen can ensure 12% of the world's total primary energy demand in 2050 [1]. Besides that, hydrogen is a valuable chemical product required for the refining industry and the production cycle of ammonia, methanol, and others. However, there is no cheap way for sustainable hydrogen production without greenhouse gas emissions.

Hydrogen can be obtained from natural gas through catalytic steam methane reforming (SMR), partial oxidation, autothermal reforming, and methane cracking. It also can be produced from water through electrolysis of water or from coal through coal gasification [2]. However, all these hydrogen production methods are very energy consuming. In addition, energy for hydrogen production is usually produced by burning hydrocarbons with carbon dioxide emissions. Most hydrogen is produced mainly via the SMR process, which also produces up to 10 kg of CO_2 per kg of generated hydrogen [3]. Greenhouse gases are produced during energy generation, as direct products of the chemical reactions, as well as during stages of compression and transportation of reagents and products. It is essential to

realize carbon capture and storage (CCS) technology to make synthesized hydrogen "blue". These actions increase the cost of hydrogen significantly [4,5].

A promising, energy-efficient, and cost-effective technology for producing low-emission (almost "green," or without any greenhouse gas emissions) hydrogen is an in situ hydrogen generation in hydrocarbon reservoirs. Hydrogen can be generated in situ in oil/bitumen fields (for example through bitumen gasification) [6–10], coal deposits (underground coal gasification) [11–13] or gas fields [14–16]. These feedstock types imply different hydrogen generation mechanisms: oil aquathermolysis and thermolysis, coke gasification, methane cracking, steam methane reforming, and water-gas shift reaction.

The chemical transformations occurring in the gas reservoir include mainly steam methane reforming, water-gas shift reaction, and methane cracking (at temperatures higher than 500 °C) in the presence of a metal-based catalyst [17,18], according to the following forward reactions:

$$CH_4 + H_2O \leftrightarrow CO + 3H_2 - 206\ kJ/mol, \quad (1)$$

$$CO + H_2O \leftrightarrow CO_2 + H_2 + 41\ kJ/mol, \quad (2)$$

$$CH_4 \leftrightarrow C + 2H_2 - 75\ kJ/mol. \quad (3)$$

At the same time, side reactions take place that consume generated hydrogen. These reactions mostly include methanation reactions: reverse reactions (1) and (3) and forward reaction [7]:

$$2CO + 2H_2 \leftrightarrow CH_4 + CO_2 + 59.0\ kcal/mol. \quad (4)$$

The generated hydrogen can be stored underground and produced at any time. Moreover, it is expected that hydrogen will rise to the geological uplifts of the reservoir under the influence of gravitational forces. Simultaneously, the environmentally undesirable greenhouse gases, such as carbon and nitrogen oxides, having a higher density than hydrogen, will sink to the bottom of the field under the influence of gravity. These gases are also more soluble in water, compared with hydrogen. In addition, carbon oxides also can react with rocks, forming insoluble compounds such as carbonates. So, greenhouse gases may not be produced at all during hydrogen production from the gas reservoir [16].

Technology considered in this study, implies pure hydrogen production from gas fields with simultaneous CO_2 storage [14,15]. It can be implemented even in depleted or abandoned fields or fields in a late stage of exploration because the main process proceeds with an increase in the amount of gaseous components (up to four volumes of hydrogen can be generated from one volume of methane). The existing infrastructure (wells, pipeline network) can be used in hydrogen production, leading to a significant decrease in the produced hydrogen cost. For example, the produced hydrogen can be transported using a modern gas pipeline through mixing with natural gas in concentrations up to 20 and even 70% (for the Nord Stream) [19].

In this research, the idea of in situ hydrogen generation within gas fields supposes the implementation of the CMC (catalytic methane conversion) in the porous medium of the reservoir. The technology implies the injection of a catalyst precursor (aqueous solution of Ni-containing salt) or an active catalyst (particles of Ni-based catalyst) into a hydrocarbon-containing zone on the first stage. Since the reducing conditions are in the reservoir, active phase of catalyst can be formed from the precursor in situ. Then the temperature in the reaction zone should be raised to a temperature, at which catalyzed SMR and methane cracking occur.

The study introduces the results of laboratory experiments performed in an autoclave reactor at initial conditions the same as in the Promyslovskoye gas field, using core material taken from this target field. The Promyslovskoye gas field is located 96 km southwest of Astrakhan city, Russia. It contains about 1700 mln m^3 of natural gas, the reservoir temperature is 48 °C, the initial pressure is 8.9 MPa, and the current reservoir pressure is 2.3 MPa. The porosity of the target layer is about 29%, residual gas saturation is 77%, and residual water saturation is 23%. The depth of gas-bearing layers is about 730 m.

The temperature range from 300 to 450 °C was discovered during the experiments to estimate the possibility of hydrogen generation from methane in situ within the target field. These temperatures can be achieved in a porous medium of rock due to steam/overheated water injection into the reservoir (up to 350 °C) or due to in situ combustion of saturating hydrocarbons (up to 700 °C for oil combustion) [20,21]. The effects of different forms of catalyst and steam/methane ratios on CMC were also investigated during the experiments. The obtained data can help conclude the expediency of the new stage of field exploration and manage the process of CMC to intensify and speed up of in situ hydrogen generation processes.

This is the first publication from the planned series of publications devoted to the in situ hydrogen generation from methane under gas reservoir conditions. The concept, feasibility, and regularities of the considered process are investigated in the current study. The results of experiments performed at more favorable conditions (higher temperature and dynamic mode) will be presented in further publications.

2. Materials and Methods

Experiments were designed to study the possibility of methane conversion into hydrogen at relatively low temperatures in the presence of different types of catalysts: in situ synthesized (precursor is nickel nitrate hexahydrate) and ex situ synthesized Ni-based. The influences of the type of porous medium and steam/methane ratio on the process were also investigated.

2.1. Porous Medium

Several different porous media were investigated, varying from crushed alumina to crushed ceramics, to river sand and crushed core. These types of porous medium simulated different types of reservoir rock, including the target gas field. Industrial alumina (Al_2O_3) pellets, Alumac 5D® (Torino, Italy), were used as an inert porous medium. Alumac 5D® has a high specific surface area of about 335 m^2/g, is very hydrophilic, inert to most liquids and gases and, is stable at temperatures up to roughly 2000 °C. Granules of Al_2O_3 were crushed to 0.8–1.2 mm before use. River sand with granules size 0.8–1.2 mm was used as filler in some experiments to model sandstone rock samples. Its composition can be roughly approximated as SiO_2. One more option for the porous medium was crushed ceramics. The mineralogical composition of this filler is presented in Table 1.

Table 1. Mineralogical composition of crushed ceramic filler.

Mineral	Value, wt.%
Mullite	68.1
Quartz	31.9

In other experiments, non-extracted core (rock) samples from the Promyslovskoye gas field were used to recreate reservoir conditions and investigate the influence of the real core on the process of hydrogen generation. The average content of total organic carbon determined with the rock-eval method [22,23] is 1.35 wt.% Data for the averaged composition of the mineral matrix is demonstrated in Table 2.

Table 2. Averaged mineralogical composition of the core for laboratory experiments.

Mineral	Value, wt.%
Albite	12.4
Anhydrite	0.8
Calcite	10.3
Halite	4.1
Illite	1.2
Pyrite	0.1
Quartz	71.1

Experimental studies observe slightly overestimated results of the methane conversion since the packed model may not exactly repeat the properties of the consolidated core. For example, the porosity and permeability of the consolidated core cannot be reproduced with high accuracy.

2.2. Catalyst Preparation Procedure

There were two types of monometallic Ni-based catalysts used in the experiments. The first one was an in situ prepared catalyst, which can be delivered into the reservoir in the form of a water solution of the catalyst precursor, then obtained through chemical transformations directly at the reservoir [24]. So, this catalyst was prepared in the reactor during experiments from catalyst precursor solution. The second one was the ex situ prepared catalyst which was nickel oxide particles supported on alumina. This catalyst can be delivered into the reservoir in the form of suspension together with steam or overheated water. In this case, the catalyst was prepared in advance and loaded into the reactor before the experiments.

The catalyst precursor, used for in situ prepared catalyst, was water-soluble nickel nitrate hexahydrate ($Ni(NO_3)_2 \cdot 6H_2O$, chemically pure), which had to be decomposed under high temperature according to the summary equation [25,26]:

$$2Ni(NO_3)_2 \cdot 6H_2O = 2NiO + O_2 + 4NO_2 + 12H_2O. \quad (5)$$

This salt solution in deionized water was put into the reactor before the experiment with other reactants (water and methane). The catalyst here is the particles of nickel oxide, which have a catalytic effect themselves or can be reduced to a more active metallic phase by interaction with hydrogen or a mixture of steam and methane at a high temperature [27–30] according to the equation:

$$NiO + H_2 = Ni + H_2O. \quad (6)$$

The second type of catalyst was the ex situ prepared catalyst by wet impregnation of α-Al_2O_3 (granular size of 0.5–1.0 mm, the specific surface area of 174 m^2/g) with a water solution of nickel salt. This catalyst was obtained through heat treatment of the carrier, and soaked in 31.42% nickel nitrate solution in a muffle furnace. Catalyst's preparing procedure included treating 100 g of α-Al_2O_3 particles with 150 g of the catalyst precursor solution (soak period-2 h), drying the carrier with the precursor solution in the air at 110 °C, while water was not evaporated. Next, the heat treatment of the carrier particles coated with precursor salt particles was necessary. Heat treatment was carried out in a muffle furnace, in the air atmosphere, for 3 h at 150 °C and then 3 h at 450 °C. The decomposition of $Ni(NO_3)_2 \cdot 6H_2O$ occurred and nickel oxide particles formed on the substrate's surface because of the last operation. The catalyst can be used in the experiments after this procedure. Such supported catalyst contains 16.16% of the active component, calculated in terms of nickel oxide.

2.3. Experimental Setup

An autoclave reactor used for static experiments is a reactor by Parr (USA), fabricated of Inconel 600 alloy, designed for experiments at max temperature 600 °C and max pressure

~408 atm. The reactor volume is 1 L. It has a control block, external heaters, magnetic stirrer, thermocouple, check valve, manometer, and bursting disc (as a safety measure). High-pressure, high-temperature tubes with the dimensions 1/8" and 1/16", and vessels by Swagelok were used for connection lines. The appearance of the reactor and hydrodynamic scheme of installation used in the experiments are shown in Figures 1 and 2, respectively.

(**a**) (**b**)

Figure 1. (**a**) The appearance of autoclave installation and (**b**) sampling system used in experiments.

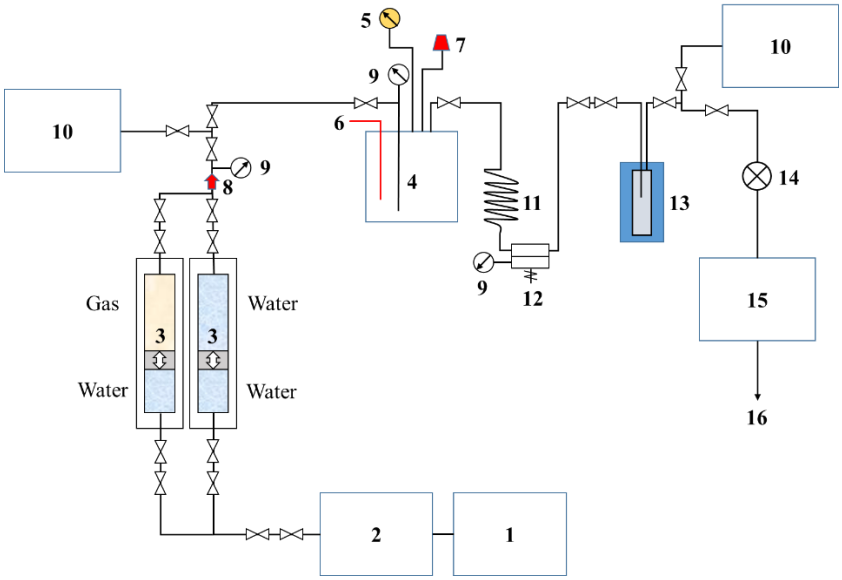

Figure 2. The scheme of autoclave installation used in experiments: 1—computer; 2—pump (Quizix); 3—piston column (V = 1 L, with gas); 4—autoclave (reactor); 5—digital pressure gauge; 6—thermocouple; 7—bursting disc; 8—check valve; 9—manometer; 10—vacuum pump; 11—condenser (cooler); 12—back pressure regulator; 13—separator (V = 0.25 L); 14—gas meter (0.5 L); 15—gas chromatograph; 16—ventilation system with gas afterburning.

2.4. Experimental Procedure

The experiments focused on studying the activity of CMC at considered conditions, the concept of in situ nanoscale active catalyst synthesis, the feasibility of CMC in the

presence of real core, and the influence of steam amount and type of porous medium on methane conversion. The set of experiments was performed by subsequently changing the type of catalyst (in situ and ex situ prepared in the form of nickel oxide), values of steam/methane ratio (from 2 to 21), temperatures (from 300 to 450 °C), and types of porous media (without filler, sandpack model, crushed ceramics, crushed alumina, and crushed core). So, the temperature of the CMC initialization, product gas composition, methane conversion rates, as well as optimal parameters for the CMC can be revealed.

In the first stage, the experimental procedure included the preparation of the catalyst (or catalyst precursor), filler for simulation of porous medium, assembly, and pressurization of autoclave installation. Then, the exact quantities of water, catalyst, and filler were placed into the reactor. After that, the whole hydrodynamic system was vacuumed, and the exact quantity of methane was injected (the quantities of loaded reagents in different tests are presented in Table 3). In the next stage, heat treatment of the reagents was performed (operational temperatures for the different tests are also presented in Table 3) with periodic gas sampling (for gas chromatography analysis by Agilent 7890 B). The experimental procedure is similar to the literature described [16].

Table 3. Reagent loads and experimental parameters.

Exp. No.	Water, mL	Methane, L	Catalyst, g	Porous Medium	T, °C
1	30.0	18.5	34.5 [1]	-	350
2	29.3	7.3	1.0 [1]	-	350–450
3	20.1	2.5	5.9	Ceramics	450
4	20.0	2.5	4.5 [1]	River sand	450
5	33.3	2.5	37.5	Alumina	450
6	42.4	2.5	5.4	Core	300–450
7	88.7	7.4	7.2	Core	450

[1] Precursor (catalyst was prepared in situ in the experiment).

If the hydrogen content in product gases is low, additional water can be injected into the reactor. This action is aimed to shift the thermodynamic equilibrium of the system to the products, as water is one of the reagents and can possibly create additional mixing of gas components. It should be noticed that water and methane are injected from the bottom of the reactor by a high-pressure pump (Quizix), and gas samples for gas chromatography analysis are taken from the top. It is also assumed that the injected water is vaporized right in front of the reactor because the inlet tube has a high temperature. At the end of the heat treatment period, the heaters of the experimental setup are turned off, the pressure decreases, and nitrogen injection begins until the reactor cools down. In the final stage, the methane conversion rate was calculated, and conclusions were made. The methane conversion rate can be calculated using the following equation, considering only the SMR process:

$$\text{Methane conversion rate } (\%) = \frac{n_{CH4,inj}(\text{mol}) - n_{CH4,rem}(\text{mol})}{n_{CH4,inj}(\text{mol})} \times 100\ \%, \quad (7)$$

where $n_{CH4,inj}$ is the amount of methane injected during the whole experimental time, and $n_{CH4,rem}$ is the amount of methane remaining after the heat treatment period and collected simultaneously with the pressure decreasing and reactor cooling down. Then the calculated value should be compared with the methane conversion rate, calculated with respect to the amount of synthesized hydrogen, directly detected on the chromatograph.

Experiment No. 1 implied heat treatment of methane and water in an autoclave at the relatively low temperature of 350 °C (Table 3). This limitation in the temperature range is determined by the maximum value that can be achieved in the reservoir by injecting steam or superheated water into the reservoir. In this experiment, in situ synthesized catalyst

was obtained in the reactor because of the decomposition of the catalyst precursor nickel nitrate hexahydrate. The experiment was carried out in the absence of a porous medium with a steam/methane ratio of 2.

Within experiment No. 2, heat treatment was performed in two stages. The first stage of heat treatment was carried out at a temperature of 350 °C, but then the temperature was increased to 450 °C. The amount of initially loaded methane was reduced. It led to an increase in the steam/methane ratio to an optimal value of five [31,32]. The amount of initially loaded catalyst precursor was also reduced. The experiment was carried out without a porous medium.

In experiment No. 3, ex situ prepared catalyst with a large specific surface area was used. At the same time, the main volume of the reactor was filled using a crushed ceramics model. In this experiment, water was not loaded into the reactor before heat treatment but was injected in several stages after the temperature had risen to 450 °C. It is believed that the injection of new portions of steam and rapid diffusion of components at this temperature ensured an even distribution of components in the pore volume of the crushed ceramics model.

In experiment No. 4, a sandpack model was used as a filler. A new attempt to synthesize an active catalyst in situ from a catalyst precursor-nickel nitrate hexahydrate, in the presence of a sandpack model at a temperature of 450 °C, was made.

Experiment No. 5 was carried out in the presence of inert alumina granules in the reactor (as a porous medium) and under conditions of an increased amount of ex situ prepared catalyst. The increased steam/methane ratio in the experiment makes it possible to create more favorable conditions for the SMR process due to the displacement of the equilibrium of the main reactions (Equations (1) and (2)) to the right, towards the products. The heat treatment of the reactor was carried out at a temperature of 450 °C. The gas sample was taken only once, at the end of the heat treatment period.

In experiments No. 6 and 7 crushed core samples from the target gas field were used to study the process of CMC in conditions close to reservoir conditions and investigate the effect of the core. Taking into account the results of previous experiments, experiment No. 6 was designed with heat treatment at two temperatures: at 300 °C and then at 450 °C, with an ex situ prepared catalyst and corepack model. In turn, experiment No. 7 repeated conditions of experiment No. 6 (with the ex situ prepared catalyst and corepack model), but was performed at lower steam/methane ratio and a heat treatment of only 450 °C.

3. Results

3.1. Determining of Thermodynamic Constraints

First of all, the thermodynamic calculations for the primary catalytic SMR process were performed. It is assumed that the SMR is the main mechanism of generating hydrogen at considered experimental conditions. Thus, this thermodynamic model is a simplification of the CMC process, which does not describe the system correctly at high temperatures (at which, for example, catalytic methane cracking occurs). At the same time, the approach overestimates methane conversion under conditions, at which other processes of hydrogen generation besides the SMR, do not yet play a significant role. It is because kinetic limitations are not taken into consideration.

The model considers only reversible reactions (Equations (1) and (2)) in a plug flow reactor for simplicity. Then, numerical methods can be used to calculate the equilibrium composition of product gases and the methane conversion rate at the reactor outlet for any values of temperature (T), pressure (p), and steam/methane ratio (ß). It is assumed that temperature and pressure are constant along the reactor's entire length. Let χ be the methane fraction converted to carbon dioxide after the whole reaction time, ξ is the methane conversion rate and K_{p1}, K_{p2} is the reaction equilibrium constants for reactions (Equations (1) and (2)), respectively. It is possible to write an expression for K_{p2} through mole fractions of hydrogen, carbon dioxide, carbon monoxide, and water (taking into account quasi-equilibrium for the reaction—Equation (2)). At the same time, these mole

fractions can be written through χ and ξ, according to the material balance equations for each chemical element and mathematical expression for χ and ξ (by definitions). Then the expression for K_{p2} could be written as:

$$K_{p2}(T) \times (\xi - \chi) \times (ß - \xi - \chi) = (3\xi + \chi) \times \chi. \quad (8)$$

The expression for K_{p1} also could be written through component's mole fractions (hydrogen, carbon monoxide, methane, and water) and overall pressure:

$$K_{p1}(T) \times (1 - \xi) \times (ß - \xi - \chi) \times (1 + ß + 2\xi)^2 = (3\xi + \chi)^3 \times (\xi - \chi) \times p^2. \quad (9)$$

If we analytically solve Equation (8) for χ, then put the answer into the Equation (9), we have the cubic equation for ξ, where $K_{p1}(T)$, $K_{p2}(T)$, ß and p are parameters. This cubic equation could be solved numerically for each value of T, p, and ß, if put here expressions for $K_{p1}(T)$ and $K_{p2}(T)$. These expressions can be written through thermodynamic functions ($_{\Delta r}G^{o}_{T}$, $_{\Delta r}H^{o}_{T}$, $_{\Delta r}S^{o}_{T}$, $_{\Delta r}C_{p}$) and approximation formulas for the reduced Gibbs energies for both of the reactions separately [33]. The result of calculating expressions for $K_{p1}(T)$ and $K_{p2}(T)$ is provided in the study [34].

In this study, the methane conversion rates and the product gas mixture's equilibrium composition were calculated using the processing of code written in the Python programming language. The calculation results for the steam/methane ratio equal to 5 are shown in Figure 3. The interval of conditions considered in experiments within this study is highlighted with a frame.

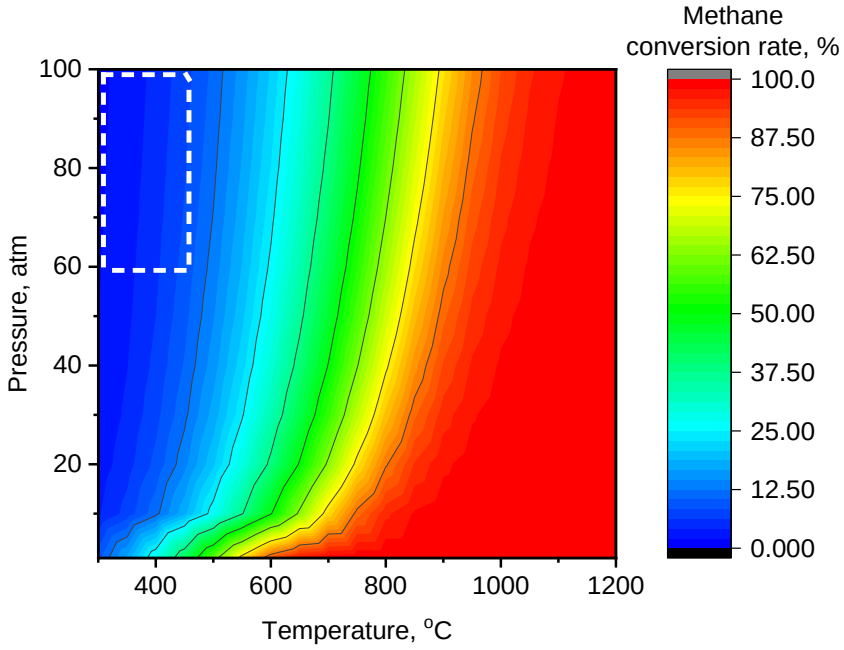

Figure 3. The dependence of methane conversion rate on temperature and pressure at constant steam/methane ratio equals 5 as a result of thermodynamic calculations for the primary catalytic SMR (steam methane reforming) process.

Also, the dependencies of methane conversion rates on temperature were plotted at various pressures (in the range from 1 to 100 atm), but at a constant steam/methane ratio of 5 (Figure 4a). They demonstrate the effect of external pressure on the catalytic SMR process. The dependencies of methane conversion rates on the temperature at various steam/methane ratios (in the range from 1 to 20) but at constant pressure 100 atm were also plotted (Figure 4b) and show the effect of additional portions of steam on the catalytic SMR process. The intervals of conditions considered in experiments within this study are highlighted with frames.

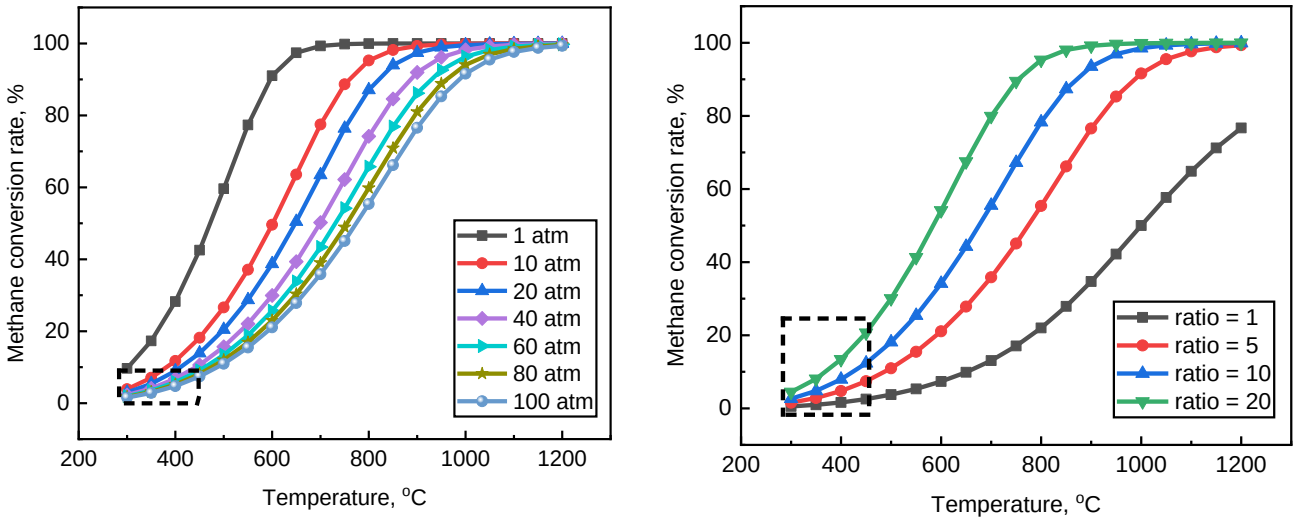

Figure 4. (**a**) The dependencies of methane conversion rates on the temperature at different pressures and constant steam/methane ratio 5 and (**b**) at different steam/methane ratios and constant pressure 100 atm, as a result of thermodynamic calculations for the primary catalytic SMR process.

Thermodynamic calculations for the SMR process allow for optimizing the experimental design and adjusting the operating parameters (initial loading of reagents, heating conditions, and others). The thermodynamic approach allows researchers an understanding of the maximum achievable methane conversion rates under specific conditions. It also provides information about the equilibrium product gas composition and about the completeness of the processes in a specific experiment. It also allows a conclusion to be made about catalyst activity, the influence of external factors, and the possible mechanism of the hydrogen generation process.

It can be seen from the obtained dependencies that the highest methane conversions are attainable at high temperatures, low pressures, and at high values of the steam/methane ratio. However, high values of steam/methane ratio and low pressures are practically unachievable in gas field conditions. One possible way of increasing the methane conversion rate is to increase the temperature inside the reservoir up to 800 °C and higher. This study describes the results of experiments, performed at relatively low temperatures, achievable in the gas reservoir due to steam or overheated water injection. In subsequent publications, the results of high-temperature experiments will be presented.

3.2. Experimental

The experimental parameters: maximum pressures in the reactor achieved during the experiments and the product gas mixture's composition for each of the experiments are shown in Table 4.

As a result of experiment No. 1, only trace amounts of hydrogen were detected in the gas samples. This may mean that the CMC is not active at the considered temperature of 350 °C, or some factors interfere with the process (for example, the active phase of the catalyst may not yet form at this temperature). However, in addition to the methane and water, significant amounts of carbon dioxide, up to 13 mol.%., and nitrogen dioxide, up to 5 mol.%., were detected in the product gases. At the same time, the methane fraction in the reactor decreased to 78 mol.%. Nitrogen monoxide and nitrogen were also detected in the product gas mixture as minor gas components.

Table 4. Summary of experimental parameters and product gas composition.

Exp. No.	Max P, atm	Max Concentration of Main Product Gas Components, mol.%.			Other Gas Components
		Hydrogen	Methane	Carbon Dioxide	
1	115	0.002	78.00	13.00	NO, NO_2, N_2
2	64	0.011	98.24	0.97	CO, NO_2, N_2
3	138	35.300	56.90	8.00	CO, C_2H_6
4	103	0.100	98.50	0.26	CO, N_2
5	120	3.100	93.00	0.40	N_2
6	207	53.500	21.42	15.67	CO, H_2S, C_2H_4, C_2H_6, C_3H_8
7	140	6.970	39.74	47.70	CO, C_2H_4, C_2H_6, C_3H_6, C_3H_8, C_4H_{10}, C_5H_{12}

The next experiment, No. 2, was optimized compared with the previous one. However, this did not lead to a significant increase in the hydrogen concentration in the reactor. The maximum achieved hydrogen fraction in the product gas mixture was only 0.011 mol.%. Simultaneously, the methane fraction in the reactor was about 98.2 mol.%, and the carbon dioxide fraction was about 1% vol. Carbon monoxide, nitrogen dioxide, and nitrogen were also detected in product gases in trace amounts. The higher temperature of heat treatment, up to 450 °C did not lead to the activation of hydrogen generation processes, since the methane concentration in the product gas mixture was almost 100%. It is more likely that the active phase of the catalyst cannot be obtained in situ with the considered conditions.

During experiment No. 3, water (steam) was injected into the reactor in several stages, with simultaneous gas composition monitoring. The maximum value of the steam/methane ratio ~10 was achieved due to additional water injections (4 injection cycles in total). As a result of the experiment, the hydrogen fraction in the product gases was about 18.5 mol.%. after one hour of heat treatment (Figure 5a).

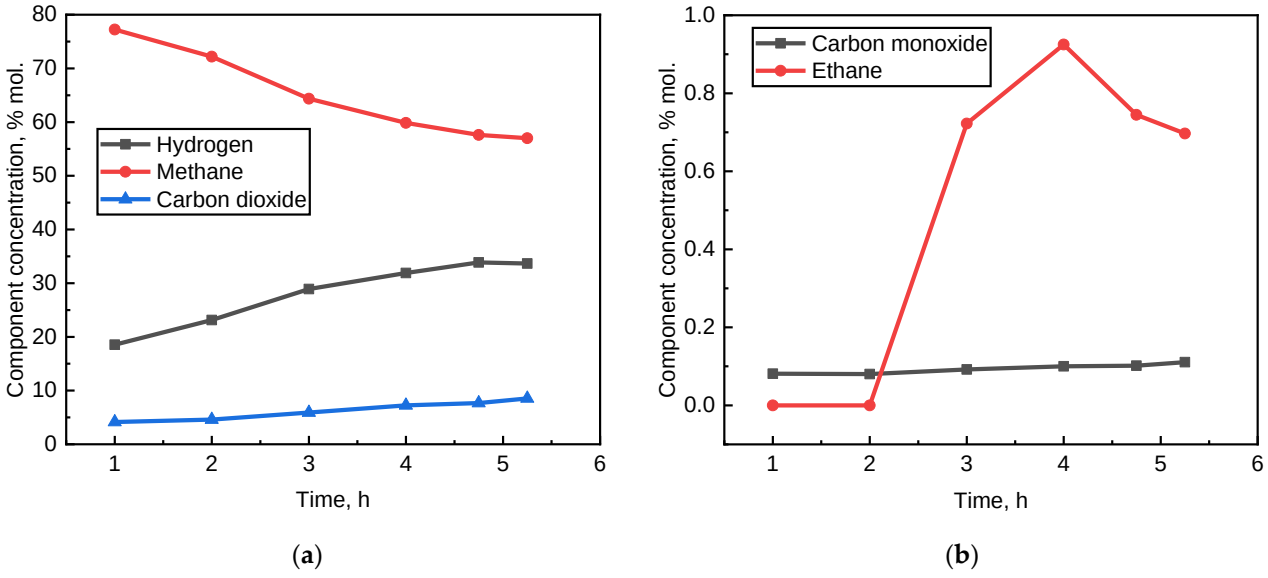

Figure 5. (**a**) The dependencies of major gas component concentrations and (**b**) minor gas component concentrations in product gas mixture in experiment No. 3 on time.

Additional portions of injected steam led to an increase of hydrogen fraction reaching the maximum value of 33.9 mol.%. The fraction of carbon dioxide in the reactor also increased consistently, up to 8.0 mol.%., and the concentration of methane decreased to ~57 mol.%. Probably, the main effects that led to a significant increase in the hydrogen concentration are the presence of a porous model in the experiment and increased values of the steam/methane ratio. Interestingly, the ethane component appeared in the reactor, with a concentration of 0.93 mol.%. The dependencies of major and minor gas component fractions in the product gas mixture on experimental time are presented in Figure 5.

The replacement of a crushed ceramics model with a sandpack model in experiment No. 4 and the loading of a catalyst precursor into the reactor instead of the ex situ prepared catalyst led to a significant decrease in hydrogen amounts. In this experiment, the Ni-based catalyst particles (nickel oxide) should have been formed from the particles of the precursor during the thermal decomposition of nickel nitrate hexahydrate, according to the reaction Equation (4). As a result of the experiment, hydrogen was detected in the product gas mixture only in trace amounts (~0.1 mol.%). At the same time, initial methane and carbon dioxide fractions almost did not change, reaching 98.5 and 0.26 mol.%., respectively.

As a result of experiment No. 5, performed in the presence of the ex situ prepared catalyst and crushed alumina, a hydrogen concentration in the product gases of 3.1 mol.%. was achieved. In this case, the steam/methane ratio in the experiment was high and equal to 17. The methane fraction in the reactor decreased to 93.0 mol.%. At the same time, the carbon dioxide fraction in the product gas mixture reached 0.4 mol.%.

Experiment No. 6 on implementing the CMC in the presence of core material from a real gas field and an ex situ prepared catalyst was carried out for almost 9 h with periodic gas sampling. In this case, the first 2 h reactor was heated to a temperature of 300 °C, and then to a temperature of 450 °C. Additional portions of water were injected into the reactor during the experiment (4 injection cycles, 42.4 mL in total), and excess pressure was released from the system if the value was higher than ~100 atm. However, these actions did not lead to activation of the CMC process. As a result of heat treatment at 300 °C, only trace amounts of hydrogen were detected in the gas samples (Figure 6a).

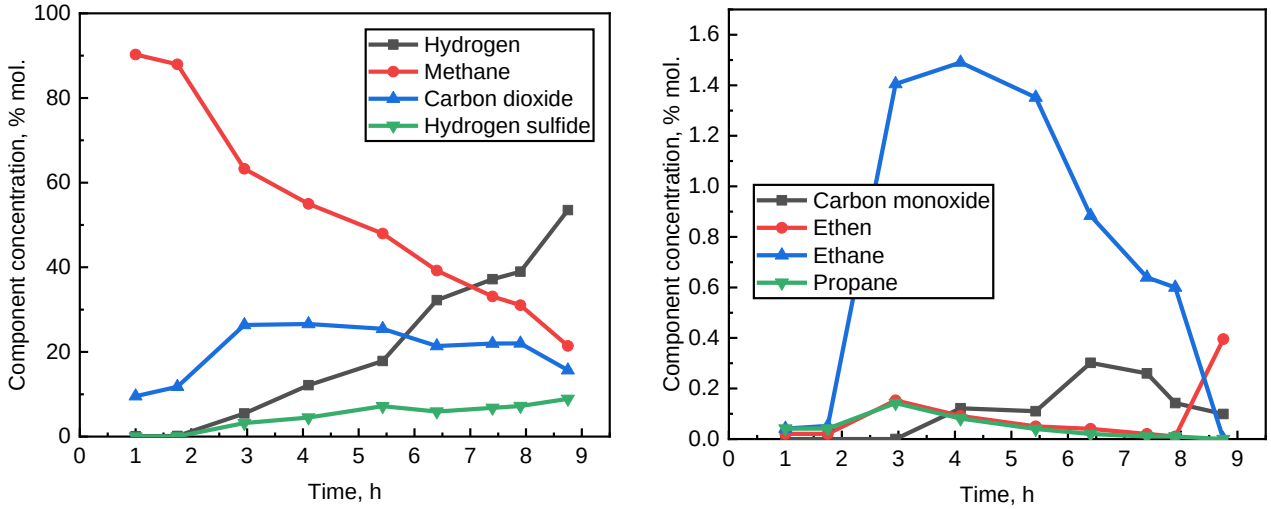

Figure 6. (**a**) The dependencies of major gas component concentrations and (**b**) minor gas component concentrations in product gas mixture in experiment No. 6 on time.

The maximum hydrogen fraction in the product gas mixture, achieved during the heat treatment at 450 °C, was 53.5 mol.%. In this case, the methane fraction in the product gas mixture was only 21.42 mol.%, and carbon dioxide was 15.67 mol.%. Hydrogen sulfide, carbon monoxide, ethane, and ethene constituted a large total fraction in the product

gas mixture. Thus, it can be concluded that some transformations occur with the core material during the experiment, which leads to the appearance of fat gas components and an increase in the concentration of carbon dioxide in the product gas mixture. The dependencies of the major and minor gas component concentrations in the product gas mixture on time are presented in Figure 6. It can be expressed from the graphs that the dependencies for the major gas components have a monotonic nature. It indicates that the system has not reached an equilibrium state at the time of the experiment completion. The methane conversion rate for the whole experiment, calculated through material balance equations, is equal to 5.80. The methane conversion rate calculated for the shorter period corresponding to the active methane conversion process is possibly much higher.

Experiment No. 7 had a similar design to experiment No. 6. However, initially, 28.6 mL of water was loaded into the reactor, then another 60.1 mL of water was injected during the heat treatment (3 injection cycles). As a result of the additional injected water, the pressure in the system rose to 153 atm. Therefore, excess pressure was released from the reactor to about 100 atm. Three pressure relief cycles were made during the whole experimental time. Even with the achievement of high values of the steam/methane ratio (up to 15), the product gas mixture contained only up to 6.97 mol.%. of hydrogen. At the same time, the methane fraction decreased to 39.74 mol.%, and the carbon dioxide fraction increased to 47.7 mol.%. The major and minor gas components' dependencies in the product gas mixture on time are presented in Figure 7. It can be expressed from the graphs that the dependencies for the major gas components reach a plateau at the end of the heat treatment period, which indicates the approach to the equilibrium state of the system. The methane conversion rate for the whole experiment, calculated through material balance equations, is equal to 3.71.

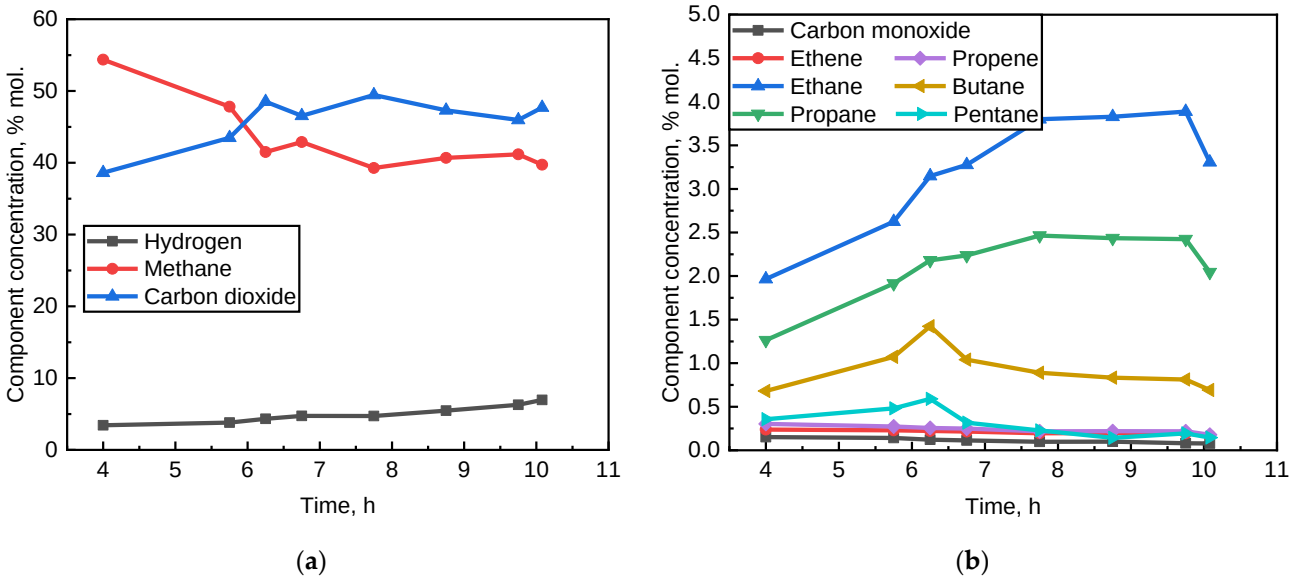

Figure 7. (**a**) The dependencies of major gas component concentrations and (**b**) minor gas component concentrations in product gas mixture in experiment No. 7 on time.

Besides the main gas components, the product gas mixture contains hydrocarbons with a carbon chain length up to C_5. Ethane was detected as a minor gas component in a concentration of up to 3.89 mol.%; ethene, up to 0.24 mol.%; propane, up to 2.46 mol.%; propene, up to 0.3 mol.%; butane and isobutane with a total concentration of up to 1.42 mol.%; and pentane, up to 0.59 mol.% (Figure 7). These components are present in the product gas mixture, most likely as a result of the organic matter of core decomposition (during the processes of thermolysis, aquathermolysis, and others).

4. Discussion

As a result of the experiments, the highest hydrogen concentration of 53.5 mol.%. was achieved in some gas samples. Although the methane conversion rate at individual stages can be quite high, the value for the whole experiment was only 5.8%. The achieved value of methane conversion is somewhat lower than those described in the literature for the SMR process carried out under similar conditions. Table 5 shows a comparative analysis of experimental data obtained by other researchers in similar methane conversion processes.

Table 5. Comparison of achieved methane conversion rate with literature data.

Catalyst	Methane Conv., %	T, °C	P, atm	Steam to Methane Ratio	Reference
10 wt.% Ni/Al_2O_3 [1]	0.0	500	1	2	[35]
10 wt.% Ni/Al_2O_3	15.0	500	1	2	
10 wt.% Ni/Al_2O_3	9.0	400	1	1	[36]
10 wt.% Ni/Al_2O_3	31.0	500	1	1	
7 wt.% Ni/Al_2O_3 + 1 wt.% Ag	75.0	500	1	4	[37]
Ni/Al_2O_3 [2]	25.0	450	1	2	[38]
10 wt.% Ni/Al_2O_3	32.0	500	1	3	[39]
16.2 wt.% Ni/Al_2O_3	5.8	450	207	21	Current study

[1] Catalyst reduction at 500 °C; [2] nanoparticle clusters.

The SMR process in the works mentioned above was carried out in a dynamic mode in continuous flow reactors, at a much lower pressure, in the presence of a catalyst previously reduced at high temperature. This study describes experiments carried out in a static mode, which imposes restrictions, for example, on the mixing of reagents. At the same time, this study describes experiments carried out simultaneously in the low-temperature and high-pressure ranges, in the presence of a core from a real gas field. Besides that, the nickel-based catalyst used in this study was activated directly in the reactor during the experiment. There was no preliminary reduction treatment stage, and the catalyst reduction took place in a steam-methane atmosphere at a temperature not higher than the experimental temperature. As a result, the hydrogen concentrations and the methane conversion rates obtained are lower than those described in the literature. The effects of temperature, the type of porous medium, and the steam to methane ratio on the catalyst activity and methane conversion are discussed below.

4.1. Applicability of Different Forms of Catalyst

In the above series of experiments, the use of two types of catalysts was considered: in situ synthesized from a water-soluble precursor-nickel nitrate hexahydrate (during the heat treatment process) and ex situ synthesized. The last type is nickel oxide particles deposited on a porous substrate from α-Al_2O_3, obtained separately from the main process.

The reason for the low hydrogen yield in experiment No. 1 may lie in the absence of an active phase of catalyst in the system. The experimental temperature of 350 °C, might be insufficient for the complete decomposition of the precursor, according to the reaction Equation (5), or for the conversion of the oxide form of the catalyst into a more active–metallic form. At the same time, the gas components NO, NO_2, and N_2 are present in the product gas mixture, indicating changes in the catalyst precursor. An excess amount of catalyst precursor was taken in the experiment in order to avoid the influence of the amount of catalyst on the activity of the process (Table 3).

Besides, a significant decrease in methane fraction from the initial 100% and an increase in the carbon dioxide fraction in the reactor should be noted. This indicates the hydrogen generation process's occurrence according to Equations (1)–(3). However, synthesized hydrogen can enter into secondary processes of catalyst or nitrogen oxides reduction.

Which is probably the main reason hydrogen was detected in experiment No. 1 only in trace amounts.

In the next experiment, No. 2, the CMC conditions were changed to determine the efficiency of the in situ prepared catalyst. An increase in temperature at the second stage of heat treatment up to 450 °C, an increase in the steam/methane ratio to 5, and a decrease in the loaded precursor amount did not allow significant methane conversion. According to the thermodynamics of the primary SMR process, an increase in temperature and steam/methane ratio leads to an increase in hydrogen concentration. Besides, a decreased amount of catalyst precursor could possibly reduce secondary reactions consuming hydrogen. Nevertheless, as in the previous experiment, only trace amounts of hydrogen were detected in the product gas mixture. In this case, the product gas consisted almost entirely of unreacted methane. The experimental results indicate the impossibility of obtaining an active catalyst in situ in the reactor during the CMC at temperatures up to 450 °C.

Experiment No. 4 was performed to look at in situ catalyst generation again by repeating successful experiment No. 3, but replacing the ex situ catalyst with the in situ one. As a result of the experiment, only trace amounts of hydrogen were obtained. However, the sandpack model could also contribute to the hydrogen yield (this influence has yet to be studied), besides the type of the catalyst.

Replacing the in situ synthesized catalyst with an ex situ prepared catalyst in experiments No. 3, 6, and 7 made it possible to obtain significant hydrogen concentrations in the product gas mixture after heat treatment of a steam-methane mixture at the temperature of 450 °C. The ex situ prepared, Ni-based catalyst supported on a porous substrate has a large specific surface area coated with nano and microparticles of nickel oxide (Figure 8). The use of an ex situ prepared catalyst ensures the oxide form of the catalyst in the reactor in the absence of nitrogen oxides.

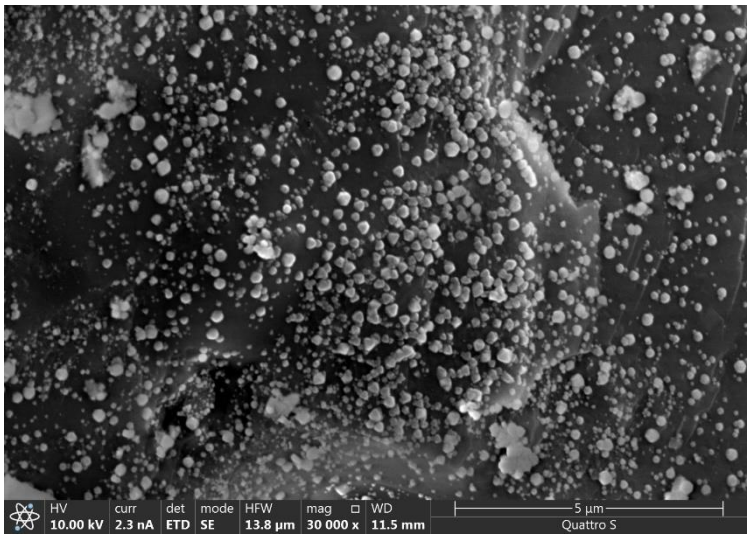

Figure 8. SEM image of ex situ prepared catalyst's surface with nickel oxide particles (light color).

Thus, experiments indicate that the active phase of the nickel-based catalyst does not form from a water-soluble nickel nitrate hexahydrate, at temperatures up to 450 °C. Other conditions or catalyst precursors should be used for active catalyst in situ generation. Nevertheless, for the implementation of the SMR process at considerable temperatures, ex situ prepared nickel-based catalyst can be used. The delivery of such a catalyst into the formation is possible in the form of a suspension, together with the injected steam or water.

4.2. Effect of Temperature on the CMC

The temperature at which the process of CMC is carried out primarily determines the process's thermodynamic constraints. A higher methane conversion rate can be achieved

with higher process temperatures (Figure 3), keeping other parameters the same. The temperature also determines in what form the catalyst could be used. For example, the insufficiently high heat treatment temperature was probably why the active phase of the catalyst was not formed during in situ in experiments No. 1 and 2. Additionally, the insufficiently high heat treatment temperature is also the reason for the hydrogen formation process's low activity.

Experiment No. 6, carried out in the presence of a real core from a gas field and an ex situ prepared catalyst, demonstrates the effect of temperature on the hydrogen generation process's activity. As a result of reagents heat treatment at 300 °C, only trace amounts of hydrogen were detected in the gas samples (Figure 6). The temperature of 300 °C is not enough for the active CMC. However, heat treatment at 450 °C led to significant hydrogen concentrations in the product gas mixture (5.47 mol.% in the first gas sample taken at a given temperature). It should be noted that the obtained high concentrations of hydrogen as a result of heat treatment at 450 °C could also be achieved with an increase of the steam/methane ratio to 21 (since temperature and steam/methane ratio were increased simultaneously) and a pressure drop. Such actions led to the shift of the thermodynamic equilibrium of the main reactions (Equations (1) and (2)), and could affect the experiment's result.

4.3. Effect of a Packed Model on the CMC

The above series of experiments also examined the effect of a porous medium composition on the CMC. Experiments were carried out in the reactor's bulk in the absence of filler, as well as in the presence of a sandpack model, crushed ceramic, crushed alumina, and a corepack model, simulating porous medium. As a result, it can be noted that significant hydrogen fractions in product gas mixtures can be obtained in the case of crushed ceramics, alumina, and core as a porous media.

For example, in experiment No. 3, the hydrogen concentration in a specific gas sample was 35.3 mol.%, and some of the ceramic granules were covered with coke (Figure 9b). This fact indicates that hydrogen generation is proceeded not only by the mechanism of the catalytic SMR but also by the mechanism of the catalytic cracking of methane (according to the reaction Equation (3)).

(**a**) (**b**)

Figure 9. (**a**) The appearance of the ceramic granules of the packed model before the experiment No. 3 and (**b**) after the experiment No. 3.

The crushed ceramics model probably contributed to the activity of hydrogen generation processes since it could contain catalyst promoters that increase catalyst activity. Probably, the crushed ceramics model also contains additional acidic catalytic sites, on

which the methane cracking reaction took place, leading to the deposition of coke on some of the granules.

Experiment No. 5 was carried out in the presence of a crushed alumina model. In this case, alumina is an inert material and pure substance of constant composition, Al_2O_3. Probably, in the absence of catalyst promoters in the packed model, the catalytic effect was significantly reduced compared with that observed in experiments No. 3, 6, 7. Therefore, the achieved hydrogen concentration in the product gases of experiment No. 5 was significantly lower than that obtained in experiments with crushed ceramics and core models. These models, which are mixtures of substances, may contain catalyst promoters (transition metal atoms), which increased catalytic effect and led to significant hydrogen concentrations.

It can also be seen from the results of gas chromatography for experiment No. 6 that the product gas mixture contains small amounts of ethane, methene, and propane. These components are cracking products (thermal cracking, hydrocracking, and aquathermolysis) of the organic matter of the core and can be detected because the core used in the experiment was not previously cleaned of the original organic matter.

Besides that, hydrogen sulfide has a significant fraction (up to 8.91 mol.%.) in the product gases in experiment No. 6. Hydrogen sulfide is most likely formed due to the decomposition of sulfur-containing components of the core (organic and inorganic) and the interaction of decomposition products with hydrogen synthesized during the experiment.

Hydrogen sulfide is also known as a catalyst poison [40] and, even in small amounts, can significantly reduce the activity of the catalyst. In turn, wet natural gas, as well as the decomposition products of the organic matter of the core, can lead to rapid coking of the catalyst, and therefore, significantly reduce the catalyst's activity. However, the experimental results indicate that the activity of the catalyst did not decrease during the experiment. This behavior can be explained by the significant concentrations of hydrogen and steam in the reactor and general reducing conditions.

Based on the results of gas chromatography for experiment No. 6, it can also be assumed that a significant contribution to the total amount of synthesized carbon dioxide was made by carbon dioxide from the core. Carbon dioxide was also formed due to the decomposition of the carbonate minerals from the core. So, the mass of the crushed core model significantly decreased. The calculation of the material balance confirms this assumption.

Similar to experiment No. 6, the carbon dioxide fraction in the product gas mixture of experiment No. 7 reaches a high value, up to 47.7 mol.%. This value is significantly higher than the equilibrium value calculated based on the SMR process's thermodynamic modeling at the considered parameters and calculated methane conversion rate. Such high carbon dioxide fraction can be explained by the decomposition of carbonate minerals of the core [41], which leads to the release of significant amounts of carbon dioxide. So, the decomposition temperature of calcium carbonate can be significantly reduced in the presence of water and carbon dioxide [42,43].

Pyrolysis results of two core samples, taken before and after experiment No. 7, confirm the previous conclusion. There is a peak on the pyrolytic spectrum corresponding to the active release of carbon dioxide from the unprocessed core sample (Figure 10, red curve). It starts at a temperature of about 450 °C at the 15th minute of heating and has a maximum at temperature of 558 °C. This peak is almost absent on the pyrolytic spectrum of the core sample taken after heat treatment during the experiment (Figure 10, green curve). The decomposition of carbonate minerals here occurs in the absence of steam and the excess pressure of carbon dioxide, which means the defined decomposition temperatures can be higher than in the real experiments.

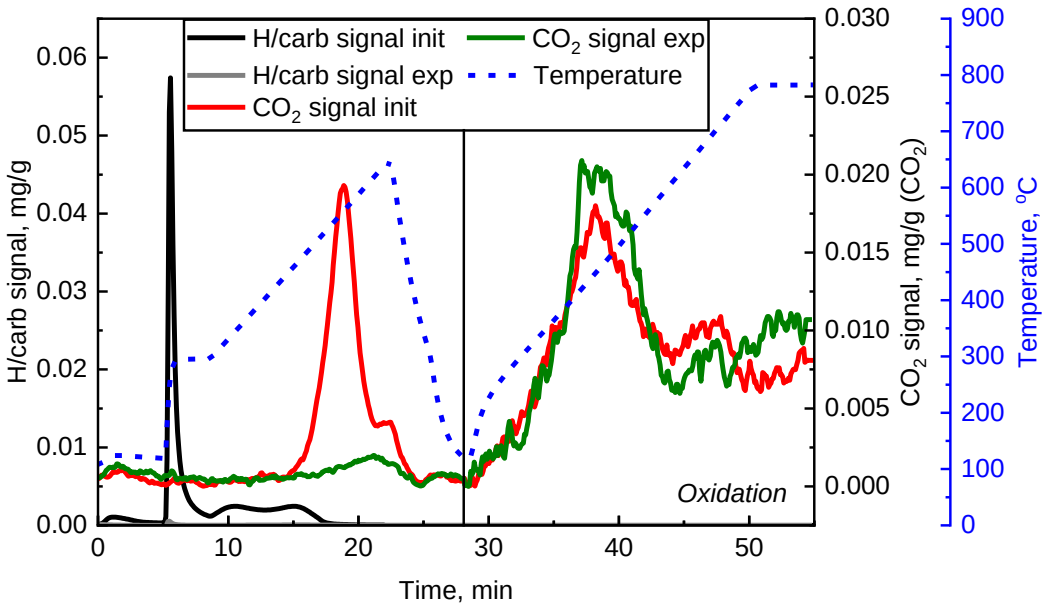

Figure 10. Pyrolytic spectra of core samples before (black and red curves) and after (grey and green curves) experiment. No. 7.

It is also seen from the pyrolysis data that the main part of the organic matter of the core decomposes in the temperature range of 135–295 °C. The curve obtained for hydrocarbons released from the core sample taken before the experiment has a peak with a maximum at a temperature of 264 °C (Figure 10, black curve). At the same time, the curve obtained for hydrocarbons from the core sample after heat treatment doesn't have this peak (Figure 10, grey curve). This fact confirms that the organic matter of the core is completely decomposed during the experiments at 450 °C.

The presence in the reactor of carbon dioxide released from the core leads to the underestimated hydrogen and other gas component fractions, compared with the equilibrium values calculated based on thermodynamic modeling and the methane conversion rate. Besides that, additional amounts of carbon dioxide in the reactor lead to a shift in the equilibrium of the main reactions of the SMR process (Equations (1) and (2)) towards the reactants, interfering with the hydrogen generation.

4.4. Effect of Steam to Methane Ratio on the CMC

Within the experiments, the amount of initially loaded water and the amount of water (steam) injected during the experiment were also changed to study the effect of the steam/methane ratio on the CMC. Based on the results of thermodynamic modeling (Figure 4b), it can be concluded that a higher methane conversion rate can be achieved with a higher amount of steam in the initial gas mixture (with an increase in the steam/methane ratio), keeping other parameters the same.

For example, the steam/methane ratio of ~10 achieved in experiment No. 3 as a result of additional water (steam) injections had a positive effect on the thermodynamic equilibrium. Additional water (steam) injections shifted the equilibrium of the main reactions (Equations (1) and (2)) towards the products and contributed to the achievement of a higher methane conversion rate, compared with experiments No. 1 and 2, in which the steam/methane ratios were 2 and 5, respectively. Additional water (steam) injections could also possibly lead to more active mixing of reagents.

A decrease in the steam/methane ratio from 21 (in experiment No. 6) to 15 (in experiment No. 7) led only to a slight decrease in the activity of the hydrogen generation processes. This conclusion can be made by comparing both experiments in terms of the calculated methane conversion rate obtained from the material balance equations for each of the components.

Considering the experimental results and thermodynamic calculations, we can conclude that the high value of the steam/methane ratio has a positive effect on the amount of synthesized hydrogen. However, providing a steam/methane ratio higher than 10 is not realistic (especially under the reservoir conditions). Nevertheless, these results confirm that the technology has great opportunities for applying in gas reservoirs with high water saturation.

4.5. Difference between Hydrogen Concentration and Methane Conversion Rate

It should be noted that the values of the gas component's fractions obtained in experiments are fair only for specific gas samples. It is better also to compare different static experiments in terms of the methane conversion rate calculated from the material balance equations for each of the components. In this case, the methane conversion rate calculations according to the detectable amounts of hydrogen should be performed. For example, the calculated value of the methane conversion rate for experiment No. 6 is 5.80%. This value corresponds to a constant equilibrium concentration of hydrogen in the reactor, about 18.8 mol.%. (based on the thermodynamic modeling of the SMR process). This value is lower than the actual observed value in some gas samples.

In experiment No. 7, product gases contained up to 6.97 mol.%. of hydrogen, and this value is much less than the value achieved in experiment No. 6 with a similar design. In turn, the methane conversion rate in experiment No. 7 is 3.71%, and this value is close to the methane conversion rate achieved in experiment No. 6. This value corresponds to the equilibrium hydrogen concentration in the product gas mixture of about 12.9 mol.%. It indicates an underestimated hydrogen concentration in gas samples (probably due to the large amounts of carbon dioxide released from the core) compared with the equilibrium value.

Thus, the results of further experiments devoted to studying the CMC process under the reservoir conditions should be compared in terms of the gas component concentrations and the calculated parameters of the methane conversion rate.

5. Conclusions

Within this study, the CMC in application to the gas reservoir for in situ hydrogen generation was investigated. A series of static experiments were then carried out in an autoclave reactor at temperatures of 300–450 °C and pressures of ~65–200 atm, representing gas field reservoir conditions under steam or overheated water injection. The effects of the heat treatment temperature, the form of catalyst used, the type of porous medium, and the steam/methane ratio on the CMC were studied. In particular, the CMC was implemented in the presence of core material, taken from the target gas field, with the initial fluid saturations representing reservoir conditions.

It was found that the CMC can be implemented under reservoir conditions in the presence of a crushed core of the target gas field at temperatures above 450 °C. At this temperature the ex situ prepared Ni-based catalyst should be used. The highest hydrogen concentration achieved during the current research was 53.5 mol.%. (in a separate gas sample), that corresponds to the methane conversion rate to hydrogen for the whole experiment of 5.8%.

Based on the obtained data and results, the following conclusions can be made:

1. The experimental results prove the activity of used Ni-based catalyst supported on Al_2O_3 substrate in the CMC. At the same time, the possibility of reducing the oxide phase of the catalyst with the formation of an active metal phase directly in the reactor during the experiment is confirmed;
2. The temperature of 350 °C is insufficient for realizing the CMC in the presence of the considered catalyst and porous media. The process becomes possible at a temperature of 450 °C, with the achievement of methane conversion rates of the order of 4–6%;
3. The packed model, which is a simulated reservoir rock, plays a key role in the process. It increases the catalytic surface area. It also includes transition metal atoms, which

can promote the main catalytic effect. Thus, the highest hydrogen concentrations were detected in experiments with crushed ceramics and crushed core models. In turn, the absence of a porous media negatively affected the hydrogen yield;

4. Based on the results of experiment No. 3, at a temperature of 450 °C, hydrogen generation from methane can occur both by the mechanism of the catalytic SMR and by the mechanism of catalytic methane cracking;
5. An ex situ prepared catalyst in an amount of 0.3 wt.% successfully catalyzed the CMC. The catalyst remained active during the whole experiment, even in the presence of relatively high amounts of hydrogen sulfide in the reactor (8.91 mol.%. in experiment No. 6);
6. The heat treatment of core material of the target gas field at the temperature of 450 °C leads to the decomposition of the mineral (carbonate) and organic matter with the release of additional amounts of carbon dioxide and light hydrocarbons, respectively;
7. An increase in the steam/methane ratio leads to a shift in the thermodynamic equilibrium of the component system towards the products and, consequently, to an increase in the amount and concentration of synthesized hydrogen. In this case, an increase in the steam/methane ratio above 10 is impractical.

The obtained results indicate the potential prospects of in situ hydrogen generation from the methane of depleted gas fields. This technology requires heating of the reservoir to 450 °C and above. It is possible due to the implementation of in situ combustion of hydrocarbons that saturate the reservoir (bitumen/oil or even natural gas). The outcomes of the dynamic high-temperature experiments showing the achievement of a methane conversion rate to hydrogen of about 40% (in the presence of crushed core material of target gas field) will be presented in following publications.

Author Contributions: Conceptualization, P.A., E.P., A.C. and R.B.; methodology, P.A., E.P., A.C. and R.B.; software, P.A.; validation, P.A., E.P., A.C. and R.B.; formal analysis, P.A.; investigation, P.A., E.P.; resources, E.M. and V.D.; data curation, P.A.; writing—original draft preparation, P.A.; writing—review and editing, E.P., A.C. and R.B.; visualization, P.A.; supervision, A.C., E.M. and V.D.; project administration, E.S., A.B., K.S. and O.S.; funding acquisition, E.M., E.S. and A.B. All authors have read and agreed to the published version of the manuscript.

Funding: This research received no external funding.

Acknowledgments: The authors would like to thank the Skolkovo Institute of Science and Technology and Integrated Center for Hydrocarbon Recovery for supporting and assisting this research. Authors thank Lukoil-Engineering LLC and Ritek LLC for providing the core material. The research was carried out in conjunction with Ritek LLC, which develops of advanced low-carbon energy technologies. The authors would like to show their gratefulness to Nikolay Taraskin, Sergey Buzov and Kirill Maerle for help in performing experiments and analyzing experimental data.

Conflicts of Interest: The authors declare no conflict of interest.

References

1. Hydrogen Council. Hydrogen Scaling Up. United Nations. 2017. Available online: https://hydrogencouncil.com/wp-content/uploads/2017/11/Hydrogen-scaling-up-Hydrogen-Council.pdf (accessed on 13 November 2017).
2. T-raissi, A. Hydrogen: Automotive fuel of the future. *IEEE Power Energy Mag.* **2004**, *2*, 40–45. [CrossRef]
3. Balcombe, P.; Speirs, J.; Johnson, E.; Martin, J.; Brandon, N.; Hawkes, A. The carbon credentials of hydrogen gas networks and supply chains. *Renew. Sustain. Energy Rev.* **2018**, *91*, 1077–1088. [CrossRef]
4. IEA. The future of Fuel: The Future of Hydrogen; France. 2019. Available online: https://iea.blob.core.windows.net/assets/9e3a3493-b9a6-4b7d-b499-7ca48e357561/The_Future_of_Hydrogen.pdf (accessed on 15 June 2019).
5. IEAGHG. Techno-Economic Evaluation of SMR Based Standalone (Merchant) Hydrogen Plant with CCS. UK. 2017. Available online: https://ieaghg.org/exco_docs/2017-02.pdf (accessed on 15 February 2017).
6. Hallam, R.J.; Hajdo, L.E.; Donnelly, J.K. Thermal Recovery of Bitumen at Wolf Lake. *SPE Reserv. Eng.* **1989**, *4*, 178–186. [CrossRef]
7. Hajdo, L.E.; Hallam, R.J.; Vorndran, L.D.L. Hydrogen Generation During In-Situ Combustion. In Proceedings of the SPE 1985 California Regional Meeting, Bakersfield, CA, USA, 27–29 March 1985; pp. 675–689. [CrossRef]

8. Kapadia, P.R.; Kallos, M.S.; Gates, I.D. A Comprehensive Kinetic Theory to Model Thermolysis, Aquathermolysis, Gasification, Combustion, and Oxidation of Athabasca Bitumen. In Proceedings of the SPE Improved Oil Recovery Symposium, Tulsa, OK, USA, 24–28 April 2010; pp. 1–31. [CrossRef]
9. Kapadia, P.R.; Kallos, M.S.; Leskiw, C.; Gates, I.D. Potential for Hydrogen Generation during In situ Combustion of Bitumen. In Proceedings of the SPE EUROPEC/EAGE Annual Conference and Exhibition, Amsterdam, The Netherlands, 8–11 June 2009; pp. 1–14. [CrossRef]
10. Kapadia, P.R.; Wang, J.J.; Kallos, M.S.; Gates, I.D. Practical process design for in situ gasification of bitumen. *Appl. Energy* **2013**, *107*, 281–296. [CrossRef]
11. Self, S.J.; Reddy, B.V.; Rosen, M.A. Review of underground coal gasification technologies and carbon capture. *Int. J. Energy Environ. Eng.* **2012**, *3*, 1–8. [CrossRef]
12. Cui, Y.; Liang, J.; Wang, Z.; Zhang, X.; Fan, C.; Wang, X.; Syngas, H.Á. Experimental forward and reverse in situ combustion gasification of lignite with production of hydrogen-rich syngas. *Int. J. Coal Sci. Technol.* **2014**, *1*, 70–80. [CrossRef]
13. Scott, E. Production of Hydrogen from Underground Coal Gasification. Patent WO 2008/033268 Al, 7 October 2008.
14. Surguchev, L.; Berenblym, R.; Dmitrievsky, A. Process for Generating Hydrogen. U.S. Patent 8763697 B2, 2014.
15. Gates, I.; Davidson, S. In-Situ Process to Produce Hydrogen from Underground Hydrocarbon Reservoirs. Patent WO 2017/136924 Al, 2017.
16. Surguchev, L.; Berenblyum, B. In-situ H_2 generation from hydrocarbons and CO_2 storage in the reservoir. In Proceedings of the Fourth EAGE CO_2 Geological Storage Workshop, Stavanger, Norway, 22–24 April 2014.
17. Zhang, Y.; Smith, K.J. Carbon formation thresholds and catalyst deactivation during CH4 decomposition on supported Co and Ni catalysts. *Catal. Lett.* **2004**, *95*, 7–12. [CrossRef]
18. Amin, A.; Epling, W.; Croiset, E. Reaction and Deactivation Rates of Methane Catalytic Cracking over Nickel. *Ind. Eng. Chem. Res.* **2011**, *50*, 12460–12470. [CrossRef]
19. Gazprom Export. Blue Fuel-Gazprom Export Global Newsletter. 48. 2018. Available online: http://www.gazpromexport.ru/files/BLUE_FUEL_48326.pdf (accessed on 18 December 2018).
20. Zhang, J.; Chen, Z. Chapter 9: Formation Damage by Thermal Methods Applied to Heavy Oil Reservoirs. In *Formation Damage during Improved Oil Recovery: Fundamentals and Applications*; Yuan, B., Wood, A.D., Eds.; Elsevier Inc.: Amsterdam, The Netherlands, 2018; ISBN 9780128137833. [CrossRef]
21. Ahmed, T.; Meehan, D.N. Chapter 6: Introduction to Enhanced Oil Recovery. In *Advanced Reservoir Management and Engineering*, 2nd ed.; Elsevier Inc.: Amsterdam, The Netherlands, 2012; pp. 541–585. ISBN 9780123855480. [CrossRef]
22. Espitalie, J.; Bordenave, M.L. Rock-Eval pyrolysis. In *Applied Petroleum Geochemistry*; Technip: Paris, France, 1993; pp. 237–361.
23. Espitalie, J.; Drouet, S.; Marquis, F. Petroleum evaluation by using the petroleum evaluation workstation (a Rock-Eval connected with computer). *Geol. Oil Gas* **1994**, *1*, 23–32.
24. Amrollahi Biyouki, A.; Hosseinpour, N.; Bahramian, A.; Vatani, A. In-situ upgrading of reservoir oils by in-situ preparation of NiO nanoparticles in thermal enhanced oil recovery processes. *Colloids Surf. A Physicochem. Eng. Asp.* **2017**, *520*, 289–300. [CrossRef]
25. Brockner, W.; Ehrhardt, C.; Gjikaj, M. Thermal decomposition of nickel nitrate hexahydrate, $Ni(NO_3)_2{\cdot}6H_2O$, in comparison to $Co(NO_3)_2{\cdot}6H_2O$ and $Ca(NO_3)_2{\cdot}4H_2O$. *Thermochim. Acta* **2007**, *456*, 64–68. [CrossRef]
26. Małecka, B.; Łącz, A.; Drozdz, E.; Małecki, A. Thermal decomposition of d-metal nitrates supported on alumina. *J. Therm. Anal. Calorim.* **2015**, *119*, 1053–1061. [CrossRef]
27. Rashidi, H.; Ebrahim, H.A.; Dabir, B. Reduction kinetics of nickel oxide by methane as reducing agent based on thermogravimetry. *Thermochim. Acta* **2013**, *561*, 41–48. [CrossRef]
28. Kharatyan, S.L.; Chatilyan, H.A.; Manukyan, K.V. Kinetics and Mechanism of Nickel Oxide Reduction by Methane. *J. Phys. Chem. C* **2019**, *123*, 21513–21521. [CrossRef]
29. Rodriguez, J.A.; Hanson, J.C.; Frenkel, A.I.; Kim, J.Y.; Pérez, M. Experimental and theoretical studies on the reaction of H2 with NiO: Role of O vacancies and mechanism for oxide reduction. *J. Am. Chem. Soc.* **2002**, *124*, 346–354. [CrossRef] [PubMed]
30. Jeangros, Q.; Hansen, T.W.; Wagner, J.B.; Damsgaard, C.D.; Dunin-Borkowski, R.E.; Hébert, C.; Van Herle, J.; Hessler-Wyser, A. Reduction of nickel oxide particles by hydrogen studied in an environmental TEM. *J. Mater. Sci.* **2013**, *48*, 2893–2907. [CrossRef]
31. Hou, K.; Hughes, R. The kinetics of methane steam reforming over a Ni/α-Al2O catalyst. *Chem. Eng. J.* **2001**, *82*, 311–328. [CrossRef]
32. Xu, J.; Froment, G.F. Methane Steam Reforming, Methanation and Water-Gas Shift: 1. Intrinsic Kinetics. *AIChE J.* **1989**, *35*, 88–96. [CrossRef]
33. Glushko, V.P.; Gurvich, L.V.; Weitz, I.V.; Medvedev, V.A.; Hachkuruzov, G.A.; Jungmann, V.S.; Bergman, G.F.; Baibuz, V.F.; Iorish, V.S. *Thermodynamic Properties of Substances in 6 Volumes*; Nauka: Moscow, Russia, 1979.
34. Zhavoronkov, N.M.; Kisil, I.M.; Olevskiy, V.M.; Kharlamov, V.V. *Nitrogenman's Handbook*, 2nd ed.; Khimia: Moscow, Russia, 1986.
35. Matsumura, Y.; Nakamori, T. Steam reforming of methane over nickel catalysts at low reaction temperature. *Appl. Catal. A Gen.* **2004**, *258*, 107–114. [CrossRef]
36. Kho, E.T.; Scott, J.; Amal, R. Ni/TiO_2 for low temperature steam reforming of methane. *Chem. Eng. Sci.* **2016**, *140*, 161–170. [CrossRef]

37. Dan, M.; Mihet, M.; Biris, A.R.; Marginean, P.; Almasan, V.; Borodi, G.; Watanabe, F.; Biris, A.S.; Lazar, M.D. Supported nickel catalysts for low temperature methane steam reforming: Comparison between metal additives and support modification. *React. Kinet. Mech. Catal.* **2012**, *105*, 173–193. [CrossRef]
38. Lai, G.H.; Lak, J.H.; Tsai, D.H. Hydrogen Production via Low-Temperature Steam-Methane Reforming Using Ni-CeO_2-Al_2O_3 Hybrid Nanoparticle Clusters as Catalysts. *ACS Appl. Energy Mater.* **2019**. [CrossRef]
39. Khzouz, M.; Gkanas, E.I. Experimental and numerical study of low temperature methane steam reforming for hydrogen production. *Catalysts* **2018**, *8*, 5. [CrossRef]
40. Rostrup-Nielsen, J.R. Sulfur poisoning. In *Progress in Catalyst Deactivation. NATO Advanced Study Institutes Series*; Figueiredo, J.L., Ed.; Martinus Nijhoff Publisher: Leiden, The Netherlands, 1982; pp. 209–227. [CrossRef]
41. Luo, Y.H.; Zhu, D.Q.; Pan, J.; Zhou, X.L. Thermal decomposition behaviour and kinetics of Xinjiang siderite ore. *Trans. Inst. Min. Metall. Sect. C Miner. Process. Extr. Metall.* **2016**, *125*, 17–25. [CrossRef]
42. Warne, S.S.J.; French, D.H. The decomposition of anhydrous carbonate minerals in coal and oil shale ashes produced at temperatures of 400 and 575 C. *Thermochim. Acta* **1984**, *75*, 139–149. [CrossRef]
43. Giammaria, G.; Lefferts, L. Catalytic effect of water on calcium carbonate decomposition. *J. CO_2 Util.* **2019**, *33*, 341–356. [CrossRef]